Folate inhibits lipid deposition via the autophagy pathway in chicken hepatocytes

Zhi-Qiang Du ⓞ,[*,†,1] Yan-Qin Pang,[*,†,1] Yu Zhang,[*,†] Li Wang,[*,†] Rong Zhang,[*,†] Hui Li,[‡] and Cai-Xia Yang[*,†,2]

[*]College of Animal Science, Yangtze University, Jingzhou, Hubei 434025, China; [†]Center of Animal Breeding Technology Innovation of Hubei Province, Wuhan, Hubei 430070, China; and [‡]College of Animal Science and Technology, Northeast Agricultural University, Harbin, Heilongjiang, China

ABSTRACT Excessive fat deposition affects the efficiency and quality of broiler meat production. To understand the molecular mechanism underlying abdominal fat content of broiler lines under divergent selection, we have attempted multiple genetics and genomics methods previously. However, the molecular mechanism of hepatic fat deposition remains largely unknown. On broiler lines divergently selected for abdominal fat content, we performed integrated mRNA and lncRNA sequencing on liver tissues. Key genes and signaling pathways related to the biosynthesis, elongation and metabolism of fatty acids, metabolic pathways, and folate biosynthesis were revealed. Then, primary hepatocytes (sex determined) were isolated and cultured, and treatment concentrations of folate and palmitic acid were optimized. Expression profiling on primary hepatocytes treated by folate and/or palmitic acid revealed that folic acid inhibited lipid deposition in a sex-dependent way, through regulating transcriptional and protein levels of genes related to DNA methylation, lipid metabolism (mTOR/SREBP-1c/PI3K), and autophagy (LAMP2/ATG5) pathways. Taken together, folate could interfere with hepatic lipid deposition possibly through the involvement of the autophagy pathway in broilers.

Key words: broiler, liver, folate, hepatocyte, lipid deposition, autophagy

INTRODUCTION

Broilers (the meat-type chicken) have been intensively selected for growth rate and feed efficiency. However, excessive fat deposition comes along, and affects broiler production efficiency and product quality (Claire D'Andre et al., 2013; Siegel, 2014; Liu et al., 2017; Kim and Voy, 2021). To study the genetic architecture and molecular mechanism underlying abdominal fat content in broiler lines under divergent selection, we previously employed integrated genetics and omics methods (Zhang et al., 2020). In chickens, liver is the major site of lipid synthesis (Noble and Cocchi, 1990) and previous work on hepatic lipid deposition at the embryo stage has been reported (Na et al., 2018). There are numerous other studies designed to reveal the molecular changes during hepatic de novo lipogenesis (Cogburn et al., 2018; Liu et al., 2020; Surugihalli et al., 2022).

Folate (vitamin B9) is stored and processed mainly in the liver (Hu et al., 2016; Zhang et al., 2021). Folic acid is closely involved in mitochondrial one-carbon metabolism, providing the methyl group important for nucleic acid methylation and synthesis, amino acid, and antioxidant homeostasis (Tibbetts and Appling, 2010; Ducker and Rabinowitz, 2017; Lyon et al., 2020; Annibal et al., 2021). Folate affects lipid metabolism in both adipose and liver tissues (Da Silva et al., 2014). In obese/diabetic mice, consumption of folic acid modulates the β-adrenoceptor-related lipolysis, and improves hepatic lipid metabolism, by up-regulating SIRT1-dependent PPARα levels, and restoring hepatic one-carbon metabolism (Lam et al., 2009; Xin et al., 2020). Maternal restrictive or excessive supplementation of folic acids all produces offsprings of increased visceral adiposity, or impaired hepatic fat metabolism (Kumar et al., 2013; Kintaka et al., 2020). High-level consumption even disturbs hepatic cholesterol homeostasis, leading to hepatocyte degeneration and liver injury (Christensen et al., 2015; Leclerc et al., 2021).

Folic acid dietary supplementation can increase folate content in eggs (Hebert et al., 2005) and potentially increase body weight gain and feed efficiency of broilers

(Rao et al., 2022; Savaram et al., 2022). Folate perfusion can decrease hepatic lipogenesis, suppress adipogenesis, and reduce abdominal fat content in broilers, the underlying molecular mechanism of which was revealed by transcriptome sequencing (Liu et al., 2019; Zhang et al., 2021). It was further discovered that paternal folate treatment could trans-generationally regulate lipid and glucose metabolism in broiler offsprings (Wu et al., 2019), as demonstrated by in ovo folate feeding experiments as well (Li et al., 2016; Liu et al., 2016). Folate can enhance proliferation, but inhibit lipid deposition of chicken preadipocytes, by increasing one-carbon metabolism-related gene expression (Yu et al., 2014). Folate also reduced triglycerides deposition in primary chicken hepatocytes (Liu et al., 2018), potentially by affecting antioxidant function and lipid metabolism (Liu et al., 2018). Fatty acid treatment on hepatocytes demonstrated the steatogenic and cytotoxic effects (Moravcová et al., 2015). Palmitic acid (**PA**) is a saturated fatty acid, the most abundant in the diet and serum as reported, and widely used in goose, mouse, human hepatocyte, and fatty liver disease studies (Pan et al., 2011; Moravcová et al., 2015; Lee et al., 2017; Zeng et al., 2020). However, the detailed molecular mechanism of folate and/or fatty acid treatments on hepatocytes remains less explored.

To investigate the molecular mechanism underlying hepatic lipid metabolism, here we performed transcriptome sequencing on livers from broiler lines divergently selected for abdominal fat content. Based on the potential involvement of folate biosynthesis in fat deposition, effects of folate and palmitic acid treatment on lipid synthesis in primary hepatocytes isolated from chicken embryos were further investigated. Folate showed sex-specific effects on expression levels of genes related to DNA methylation, lipid metabolism, and also autophagy. Protein abundances related to autophagy (LAMP2 and ATG5) and lipid synthesis (mTOR and SREBP-1c) were also evaluated.

MATERIALS AND METHODS

Experimental Animals

Broiler lines under divergent selection for abdominal fat content at Northeast Agricultural University (**NEAUHLF**) were used, and striking difference existed between the fat and lean broiler lines (Na et al., 2018; Zhang et al., 2020). Liver tissues from 10 birds at 7 wk of age (5 for each line) at generation 19 were used for transcriptome sequencing (lncRNA and mRNA).

RNA-Seq

Total RNAs for all tissues and cells were extracted using 1 mL Trizol Reagent (Invitrogen Life Technologies, Carlsbad, CA) according to the manufacturer's instructions. Briefly, hepatic tissues from 10 birds were used, and after quality control, a total of 3 μg RNA per sample was submitted as the input materials for lncRNA and mRNA sequencing. Ribosomal RNAs were removed by the Epicentre Ribo-zero rRNA Removal Kit (Epicentre, Madison, WI).

Sequencing libraries were constructed by the NEBNext Ultra Directional RNA Library Prep Kit for Illumina (NEB, Ipswich, MA) following the manufacturer's recommendations. Using divalent cations under elevated temperature in NEBNext First Strand Synthesis Reaction Buffer (5X), fragmentation was carried out, and the first-strand cDNA was synthesized, using random hexamer primers. M-MuLV Reverse Transcriptase DNA Polymerase I and RNase H were added to synthesize the second-strand cDNA. Overhangs were converted into blunt ends via exonuclease/polymerase activities, and adenylation of 3′ ends of DNA fragments was performed. Then, ligation of NEBNext Adaptors with hairpin loop structure was done for hybridization. Fragments of 350 bp were purified with the AMPure XP system (Beckman Coulter, Beverly), and 3 μL USER Enzyme (NEB, USA) was used with size-selected, adaptor-ligated cDNA at 37°C for 15 min, followed by 5 min at 95°C, before performing PCR with Phusion High-Fidelity DNA polymerase, Universal PCR primers and Index (X) Primers. PCR products were purified (AMPure XP system), and the clustering of the index-coded samples was performed on a cBot Cluster Generation System using the TruSeq PE Cluster Kit v3-cBot-HS (Illumina, San Diego, CA) according to the manufacturer's instructions. Library quality was checked on the Agilent Bioanalyzer 2100 system, and sequenced on the Illumina Hiseq 4000 platform, to generate 150 bp paired-end reads.

Clean reads were obtained by removing raw reads containing adapter, reads containing poly-N, and low-quality reads, and Q20, Q30, and GC contents were calculated. Reference genome and transcript annotation files (Galgal 6.0) were downloaded directly from Ensembl (http://www.ensembl.org/index.html). Bowtie2 and TopHat v2.0.9 were used to align the paired-end clean reads to the reference genome (Trapnell et al., 2009; Langdon, 2015). The mapped reads were assembled by Cufflinks (v2.1.1) in a reference-based approach (Trapnell et al., 2012). Cuffdiff was used to determine transcripts or genes with a P-adjust <0.05 to be significantly differentially expressed.

Coding Potential Calculator (**CPC**) (Wang et al., 2013) and phylogenetic codon substitution frequency (**PhyloCSF**) (Lin et al., 2011) were used to predict transcripts without coding potential as candidate lncRNAs. Gene ontology (**GO**) and Kyoto Encyclopedia of Genes and Genomes (**KEGG**) pathway analyses were conducted using DAVID (Huang da et al., 2009), to analyze the cellular component, molecular function, and biological process of mRNAs targeted by DE lncRNAs. Although lncRNA may have regulatory effects on nearby protein-coding genes, target mRNAs were selected by setting the co-location threshold to 100 kb upstream and downstream of lncRNAs.

Primary Hepatocyte Isolation and Culture

Eggs from Arbor Acres (**AA**) broiler breeders were incubated according to the standard procedure. On embryonic day (**ED**) 14, livers were dissected from embryos, and washed 3 times with precold D-PBS solution. Sexing was performed by examining the sexual gland. Hepatic tissues were cut into 0.5 to 1 mm^3 pieces, washed three times with cold D-PBS solution again, and then, mixed with 0.12% Collagenase Type II solution, kept at 37°C for 10 min. Red blood cells were treated with the lysis solution (139.6 mM NH_4Cl, 16.96 mM Tris, and pH calibrated to 7.2 by 1 M HCl). After filtering, supernatant was centrifuged at 1000 r/min for 5 min, and cells at the upper level in yellow were hepatocytes. Hepatocytes were transferred into the Leibovitz's L-15 adherent medium (10% fetal bovine serum, 10 μg/mL human transferrin, 10 μg/mL vitamin C, 10-6 M dexamethasone, 5 μg/mL bovine insulin, 100 U/mL penicillin, and 100 μg/mL streptomycin). Hepatocytes at 1×10^6 cell/mL were seeded in 6-well plates, and cultured at 37°C and 100% humidity. After 24 h, the basal medium was replaced to continue culture (removal of fetal bovine serum).

Hepatocyte Glycogen Content, Viability, and Activity Test

To detect the glycogen content, the Periodic Acid-Schiff (**PAS**) kit (D004-1-2, Nanjin, China) was used according to the manufacturer's protocol. Equal amount of 0.4% Trypan Blue solution was mixed with cell suspension, and live and dead hepatocytes were counted, to calculate the cell viability rate. Activity of lactate dehydrogenase (**LDH**) was assayed using the LDH kit (A020-2-2, Nanjin, China) according to the manufacturer's protocol.

Folate and Palmitic Acid Treatments

Screening of optimal folic acid and palmitic acid concentrations were performed. After 24 h treatment, culture media were collected to test the hepatocyte LDH activity, continuously from day 2 to day 7. Folate at 5 concentrations (0, 5, 10, 15, and 20 μM) were used, 6 replicates for each concentration. For palmitic acid, 5 preliminary concentrations (0, 50, 75, 100, and 125 μM) were used, also 6 replicates for each concentration. Next, 6 concentrations (0, 10, 20, 30, 40, and 50 μM) were set, to find the optimal concentration.

Oil Red O Staining

Cells were washed 2 times with cold PBS, and fixed for 30 min by 4% paraformaldehyde solution. In each well, 500 μL Oil red O were added, and incubated in dark at 37°C for 20 min. Then, we discarded Oil red O dye, added 500 μL 60% isopropyl alcohol to each well, discarded isopropyl alcohol after 15 s, and rinsed with 1 × PBS 3 times. Cells were viewed under a microscope and photographed. Next, PBS was discarded, added 100% isopropyl alcohol to dissolve Oil red O, and measurement was performed at 510 nm.

Quantitative Real-Time PCR

Total RNAs for primary hepatocytes were extracted using the Trizol reagent (Invitrogen Life Technologies, Carlsbad, CA). Reverse transcription was performed, and qRT-PCR was done on a 7500 Real-Time PCR System (Applied Biosystems, Carlsbad, CA), using the Roche FastStart Universal SYBR Green Master Mix (Roche Molecular Systems, Basel, Switzerland) (Primer sequences in Additional file 1: Table S1). GAPDH was chosen as the internal control, and the relative quantitative ΔCt method was used for differential expression analysis.

Western Blots

Hepatocyte samples were treated with RIPA Lysis Buffer (Beyotime, Shanghai, China). Proteins quantified using BCA Protein Assay Kit (Beyotime, Shanghai, China) were separated by SDS-PAGE and transferred onto PVDF membranes (Beyotime, Shanghai, China). The membranes were blocked with 5% skimmed milk/ 5% BSA in phosphate buffer solution with Tween-20 (PBST) for 1 h and then incubated with antibody against mTOR (AP0115, ABclonal, Boston, MA), SREBP-1c (14088-1-AP, Proteintech, Chicago, IL), LAMP2 (66301-1-Ig, Proteintech), ATG5 (A0203, ABclonal), or β-actin (20657-1-AP, Proteintech) overnight at 4°C. On next day, membranes were probed with an HRP-conjugated secondary antibody (ZSGB-BIO, Beijing, China). Target protein bands were visualized using BeyoECL Plus kit (Beyotime, Shanghai, China), and quantified with ImageJ (NIH, Bethesda, MD).

Statistical Analysis

All results were expressed as mean ± SEM, and analyzed by the Student's t test, or ANOVA using SPSS 19.0 (SPSS Inc., Chicago, IL). Differences were considered to be statistically significant at * ($P < 0.05$), ** ($P < 0.01$), and *** ($P < 0.001$) levels.

RESULTS

Transcriptome Sequencing of Liver Tissues

To further investigate the molecular mechanism of hepatic lipid metabolism, and help better understand the strikingly different abdominal fat deposition between broiler lines under divergent selection, transcriptome profiling (both mRNA and lncRNA) on chicken livers was conducted. A total of 722 significantly differentially expressed mRNAs (444 up-regulated and 278 down-regulated, respectively) were found (Figure 1A). Gene enrichment analysis
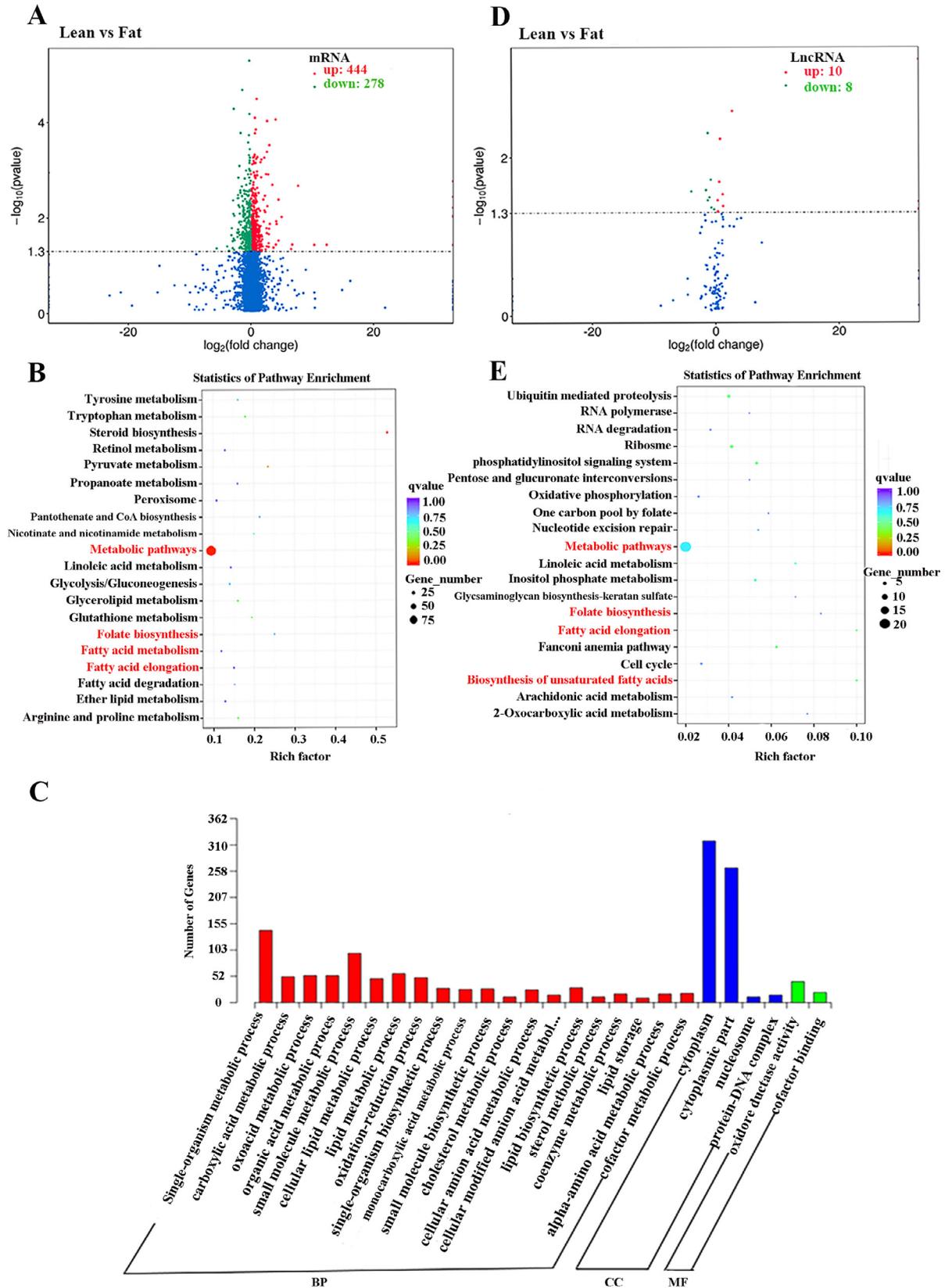
Figure 1. Differentially expressed mRNAs and lncRNAs, and gene enrichment analyses (GO and KEGG). (A) Volcano plot of differentially expressed mRNAs (DEMs). (B) KEGG pathway analysis of DEMs. (C) Gene ontology (GO) analysis. (D) Volcano plot of differentially expressed lncRNAs (DELs). (E) KEGG pathway analysis of genes targeted by DELs.

identified a number of signaling pathways, such as fatty acid metabolism and elongation, folate biosynthesis and metabolic pathways (KEGG pathway, Figure 1B), and lipid, sterol, cofactor, and coenzyme

metabolic processes (GO, Figure 1C). Moreover, 102 novel lncRNAs were characterized, to be without coding potential, relatively short, with less numbers of exons and typical pattern of genomic distribution

A

B

C
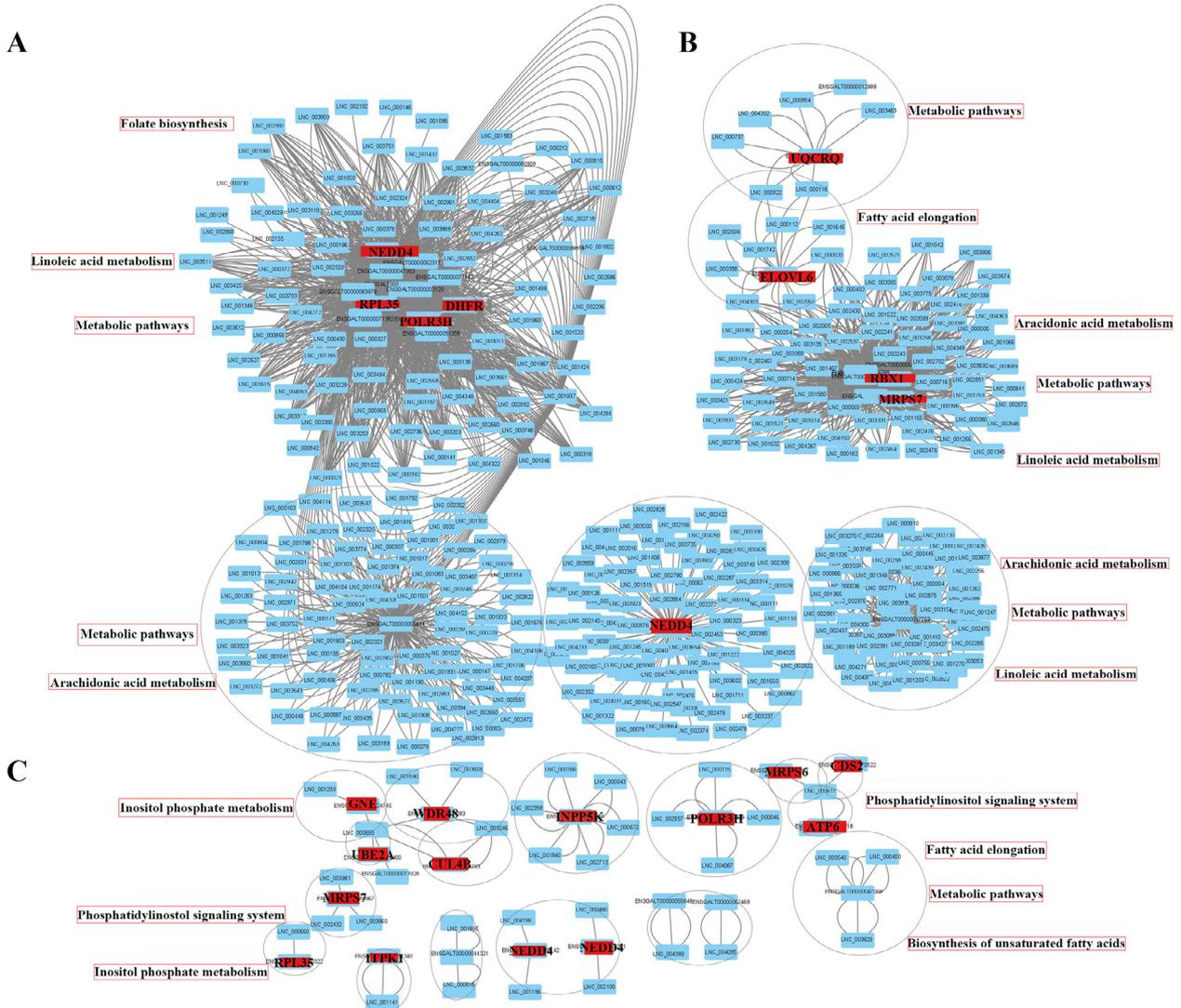
Figure 2. Integrative lncRNA and mRNA network analysis. (A) The largest sub-network, with hub genes (NEDD4 and DHFR) and signaling pathways (folate biosynthesis, fatty acid metabolism, and metabolic pathways) identified. (B) The second largest sub-network, with hub gene ELOVL6, and fatty acid metabolism and metabolic pathways. (C) Multiple small sub-networks. In all sub-networks, mRNAs were positioned in the middle, and surrounded by lncRNAs.

(Additional file 2: Figures S1A−S1D), of which 18 were significantly differentially expressed (10 up- and 8 down-regulated, Figure 1D). After KEGG pathway analysis, enrichment of fatty acid metabolism and elongation, folate biosynthesis, and metabolic pathways were also found (Figure 1E). Furthermore, both significantly differentially expressed mRNAs and lncRNAs could clearly cluster the liver samples into 2 groups (Additional file 2: Figures S1E−S1F). Integrative lncRNA and mRNA network analysis revealed hub genes and signaling pathways related to the biosynthesis, elongation and metabolism of fatty acids, metabolic pathways, and folate biosynthesis (Figure 2). Expression levels (FPKM) of genes related to folate and lipid metabolism were retrieved from hepatic RNA-seq data, significantly different between the fat and lean broiler lines (Additional file 3: Figure S2). Therefore, apart from other signaling pathways, folate biosynthesis could be related to hepatic lipid metabolism in broilers.

Folate and Palmitic Acid Treatments on Primary Hepatocytes

To understand how folate affects hepatic lipid deposition, we further cultured primary hepatocytes, isolated from single broiler embryos and examined the effects of folic acid (**FA**) and/or palmitic acid (**PA**) treatments on hepatocytes. Hepatocytes were sexed by checking sexual glands for each embryo. Morphology and characteristics of hepatocytes were examined by PAS staining and LDH activity assays (Additional file 4: Figure S3). The optimal FA concentration (15 μM) was determined by treating hepatocytes with 5 concentrations (0, 5, 10, 15, and 20 μM), and then measuring the LDH activity (highest at 15 μM) (Additional file 5: Figure S4). A preliminary 5 concentrations (0, 50, 75, 100, and 125 μM) were set for PA, and at 50 μM, LDH activity was found to be the highest (Additional file 6: Figure S5). Then, in the range of 0−50 μM, another 5 concentrations (10, 20, 30, 40, and 50 μM) were set, and 40 μM was found to be

A

B
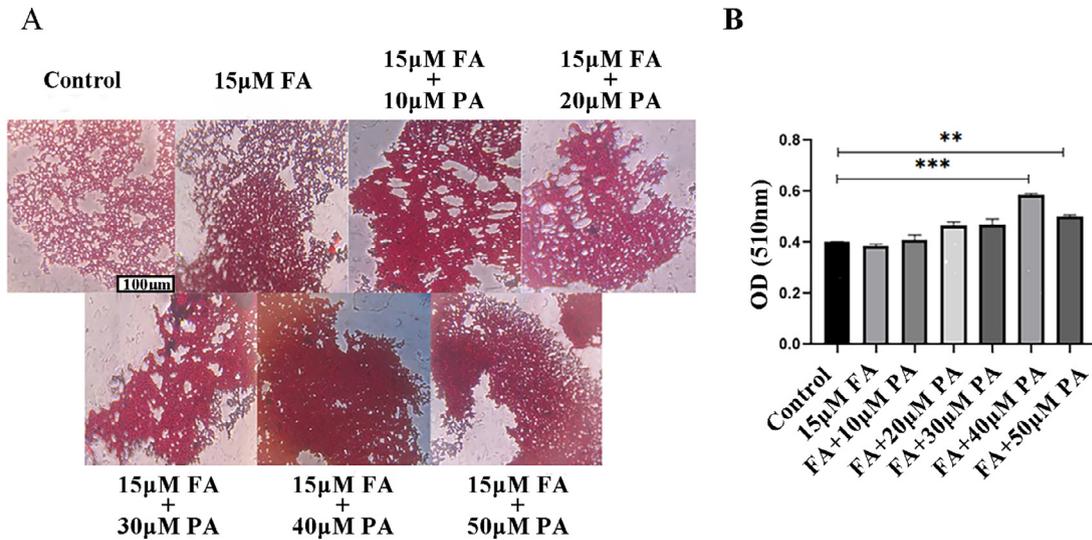
Figure 3. Optimal concentrations of folate and palmitic acid treatment on primary hepatocytes. (A) Oil red O staining. (B) OD values of different concentration combinations.

the optimal concentration. Furthermore, the effect of PA treatment on hepatocytes was checked by the Oil red O assay, and 40 μM PA was also found to have the largest number of lipid droplets (Additional file 7: Figure S6). Combined treatments of FA and PA on hepatocytes were also assayed, which gave the optimal combination of 15 μM FA + 40 μM PA (Figure 3).

Gene Expression Profiling

Sex-specific effects of FA and/or PA treatment were found for most of the genes examined. First, expression levels of the folate transporter PCFT and key metabolism enzyme DHFR (Crider et al., 2012), DNA methylation-related genes (MTHFD2, MTHFR, and DNMT1), and 2 genes (GCK and PGC-1α) related to glucose and energy metabolism were examined (Figure 4). FA treatment significantly increased PCFT levels, and additional PA supplementation only slightly modified the expression trend (Figure 4A). However, DHFR seemed to have sex-specific response to FA/PA treatments, and until day 4, expression level significantly increased in female hepatocytes. FA seemed to have also sex-specific effects on the expression of DNA methylation-related genes (Figure 4B). FA treatment could significantly increase the expression levels of MTHFD2 and MTHFR in males and females, respectively, but DNMT1 in both sexes. Further PA supplementation seemed to suppress their expression levels. Moreover, GCK levels in both sexes decreased significantly, whereas PGC-1α increased its expression level significantly by FA treatment (Figure 4C). Additional PA treatments further significantly increased their expression levels.

Next, although GCK and PGC-1α significantly changed their expression levels when treated by FA and PA, indicating lipid metabolism might be involved, we further profiled genes related to lipid synthesis and lipolysis. For genes related to lipid synthesis, FA treatment

had different effects on females and males, relatively higher in males (Figure 5A). FA could elevate FAS but inhibit ACC expression levels significantly in both female and male hepatocytes, and suppress SCD in males, but ELOVL6 in females, with highly significant effects, respectively. Simultaneous FA + PA treatments only affected FAS and ACC expression levels in males, inhibited significantly SCD expression, and had nearly no effect on ELOVL6.

In contrast, for genes related to lipolysis, FA treatment seemed to increase expression levels of FABP1, CREB, PPARα, and ACOX1, significantly for all male hepatocytes, and for CREB in female hepatocytes, too (Figure 5B). Further addition of PA didn't change further their expression patterns.

mTOR-SREBP1-PI3K and Autophagy Pathways

Although expression patterns of genes related to lipid metabolism showed significant difference, we evaluated first the mTOR-SREBP-1-PI3K pathway, fundamentally involved in the regulation of nutrient metabolism. Gene expression demonstrated that FA could highly significantly enhance the levels of mTOR, SREBP-1c, and PI3K in both male and female hepatocytes (Figure 6A). Co-treatments with PA suppressed significantly the expression levels of mTOR and PI3K expression, but enhance that of SREBP-1c. Furthermore, protein concentrations of female hepatocytes treated by FA and FA + PA were quantified, respectively (Additional file 8: Figure S7). Western blots on mTOR and SREBP-1c in female hepatocytes further confirmed their significantly elevated protein abundances, similar to their gene expression patterns (Figures 6B and 6C).

As for the autophagy pathway, we profiled transcriptional levels of ATG5 and LAMP2, and found
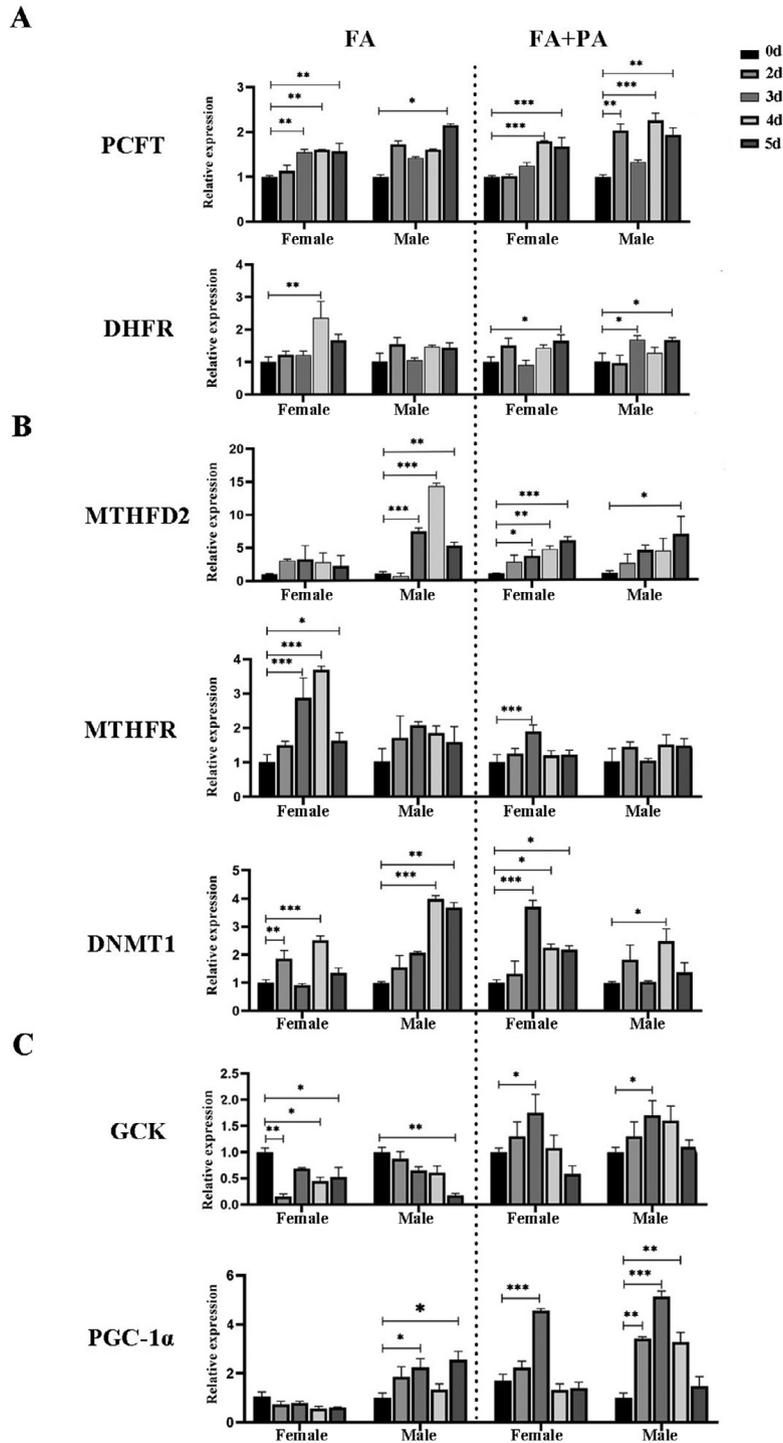
Figure 4. Expression profiling of genes in hepatocytes. (A) Folate transporters. (B) Folate metabolism and DNA methylation. (C) Lipid metabolism.

that FA treatment could significantly enhance ATG5 expression in females, and LAMP2 expression in both females and males (Figure 7A). Further PA treatment increased highly significantly the expression level of ATG5, but not for LAMP2, of which the significance level was not changed. Western blotting analysis confirmed the significantly elevated levels of ATG5 and LAMP2 (FA + PA treatments on female hepatocytes), with a pattern similar to their gene expression dynamics (Figure 7B).

DISCUSSION

The liver is the major organ for folate metabolism and lipogenesis in chickens (Noble and Cocchi, 1990; Zhang et al., 2021). Abdominal fat deposition is a complex trait, under the regulation of multiple genetic and environmental factors. Using the broiler lines under divergent selection for abdominal fat content, we attempted to understand the genetic underpinnings through a combination of molecular, genetic, and

DU ET AL.
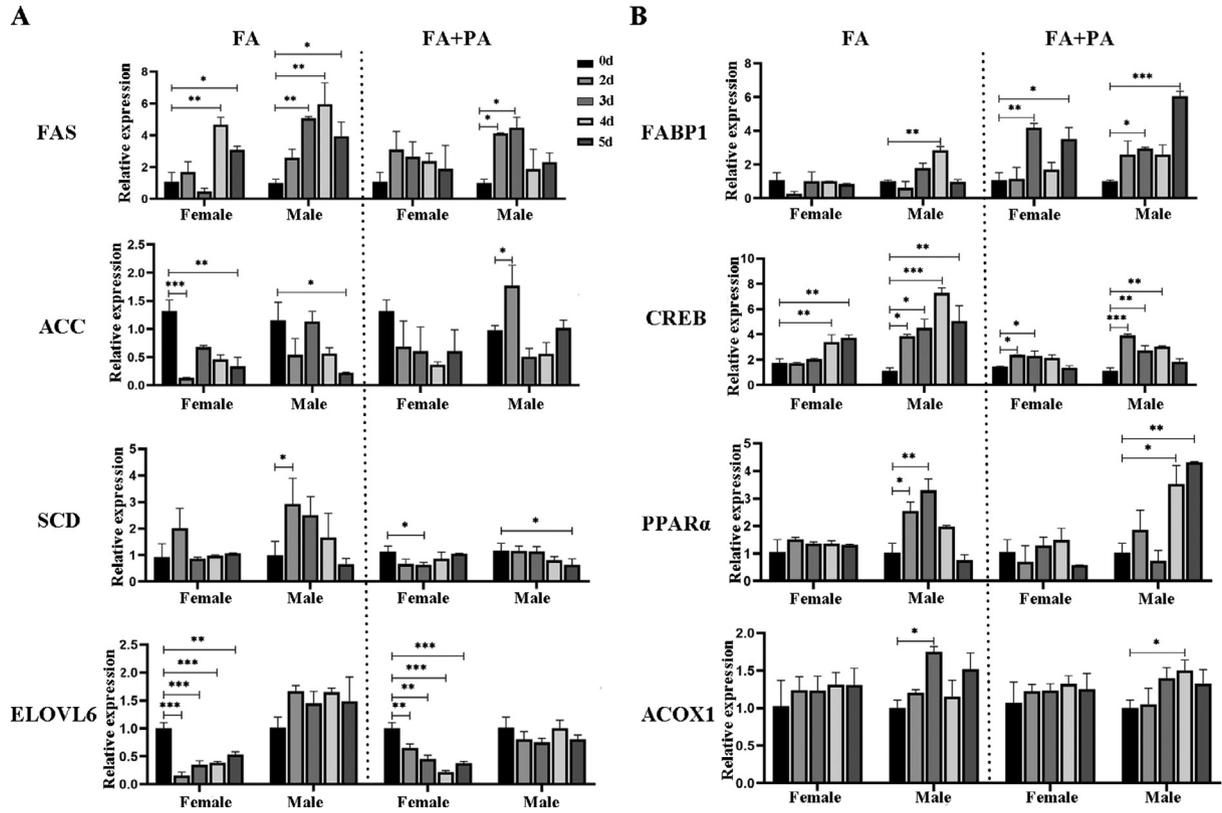
Figure 5. Gene expression profiles related to lipogenesis after folate and/or palmitic acid treatments. (A) Lipid synthesis. (B) Lipid catabolism.
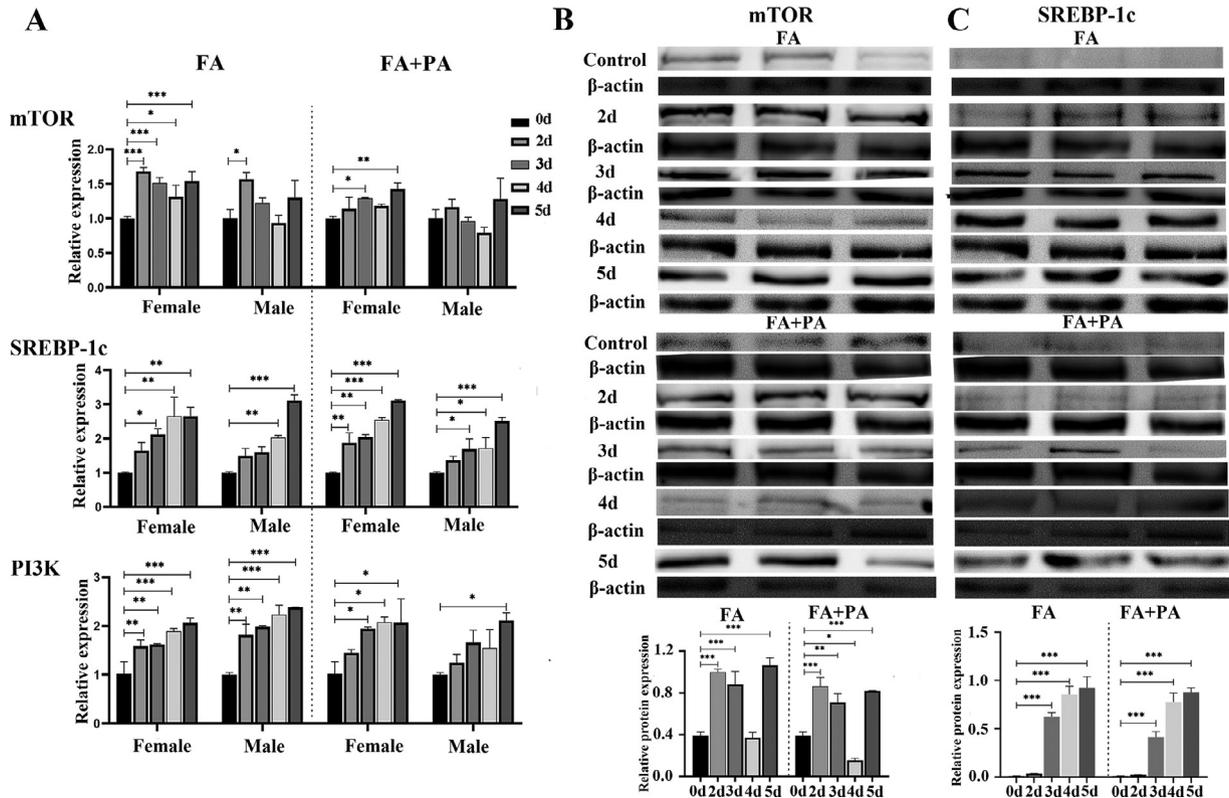
Figure 6. The mTOR-SREBP-1c-PI3K pathway. (A) Expression profiling. Western blots on mTOR (B) and SREBP-1c (C) in female hepatocytes.
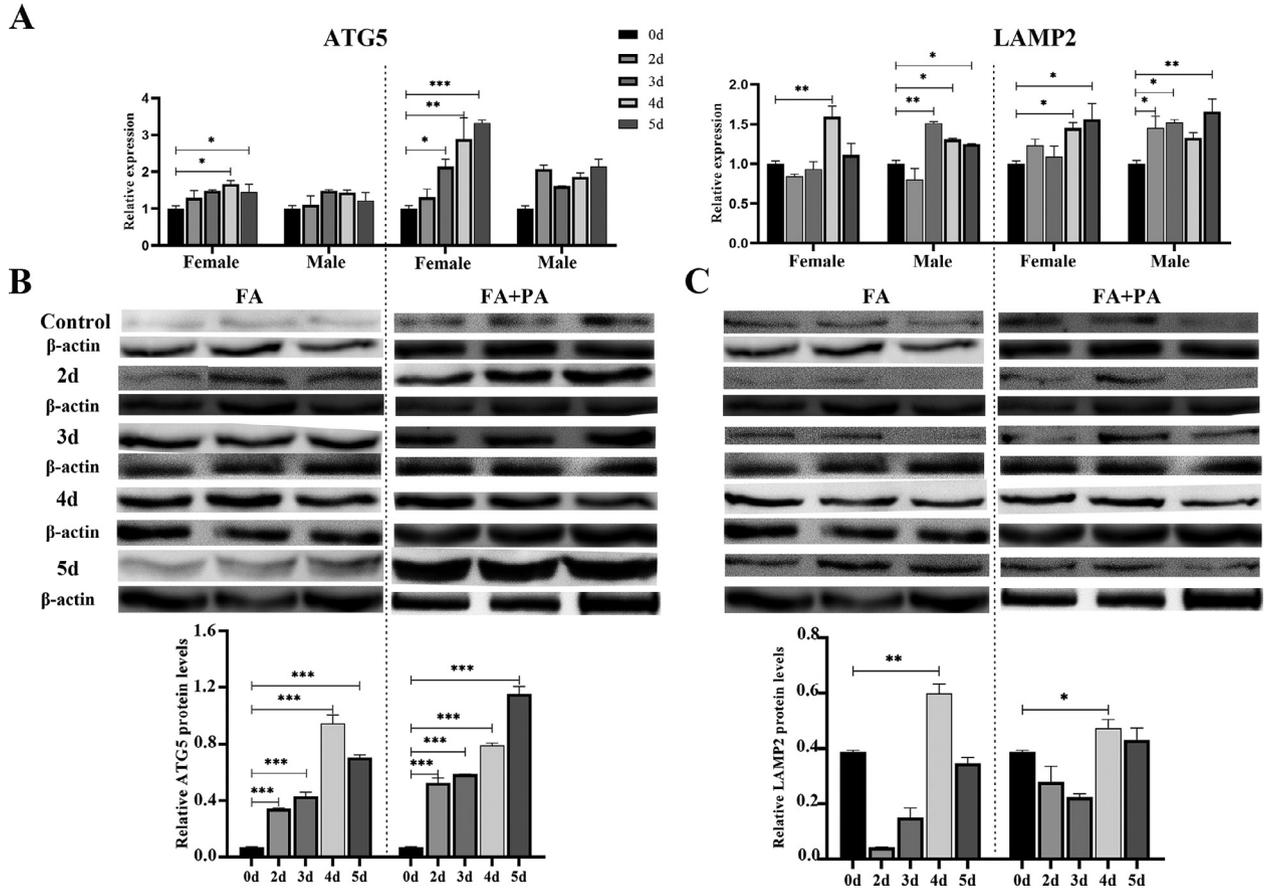
Figure 7. The autophagy pathway. (A) Transcriptional profiling on ATG5 and LAMP2. (B) Western blots on ATG5 (B) and LAMP2 (C) in female hepatocytes.

quantitative efforts (Na et al., 2018; Zhang et al., 2020). Through liver transcriptome sequencing, in the present study, we found that besides a number of other signaling pathways, folate biosynthesis could be important to lipogenesis.

PCFT, the newly discovered folate transporter, is in charge of the intracellular FA homeostasis (Crider et al., 2012), and found here to be highly expressed after FA supplementation. For FA metabolism, three key enzymes (DHFR, reduction of dietary folic acid or dihydrofolate to tetrahydrofolic acid (**THF**); MTHFR, irreversible conversion of 5,10-methylenetetrahydrofolate to 5-methyltetrahydrofolate; and MTHFD2, catalyzing the NAD+ dependent 5,10-methylene-THF dehydrogenase and 5,10-methenyl-THF cyclohydrolase reactions within the mitochondria) were also disturbed (Tibbetts and Appling, 2010; Zhang et al., 2021). In addition, as a methyl donor, FA supplementation affected DNMT1 expression, in line with previous reports that FA participates in DNA and RNA methylation, and epigenetic regulation (Crider et al., 2012). Furthermore, FA seems to have sex-specific regulatory effects on gene expression as found in the present study, which provides additional information on maternal FA supplementation and its effect on embryo development (Fan et al., 2021). Though research interests on sex-specific phenomena have been brought into attention, the underlying molecular mechanism still awaits further investigation.

Folate deficiency or over-supplementation could have detrimental effects (Kumar et al., 2013; Kintaka et al., 2020). Folic acid increased the expression of LPL and IGF2 genes and decreased the methylation level of IGF2 gene in liver of broilers (Liu et al., 2018). A previous transcriptome sequencing study found that folate treatment reduced not only PPARγ and FAS expression levels, and lipid droplets in abdominal fat, but also LPL, PPARγ, and FAS protein levels in livers (Zhang et al., 2021; Surugihalli et al., 2022). In addition, signaling pathways associated with folate biosynthesis, PPAR signaling pathway, TGF-beta were also enriched (Zhang et al., 2021). Here, we profiled the expression dynamics of genes related to lipid synthesis and lysis on hepatocytes treated by folate, also indicating lipid deposition was suppressed. These results suggest that folic acid could potentially regulate lipid metabolism, but the detailed molecular mechanism remains to be studied.

Autophagy is recently discovered to be involved in lipid metabolism, and since has been extensively studied (Kouroumalis et al., 2021; Trivedi et al., 2021). Here, we found that mTOR (the key regulator of nutrient and energy metabolism) and the downstream SREBP-1-PI3K and ATG2/LAMP2 (autophagy effectors) pathways were disturbed by folate treatment on hepatocytes. The primary role of autophagy is as an important component of the recycling system, elimination of unwanted

materials (metabolites, organelles, etc.) and renovation/rejuvenation of cellular building blocks (Kouroumalis et al., 2021). Autophagy is also found to be implicated in regulation of metabolism (e.g., lipid, sugar, and amino acid), and fundamental to hepatic lipogenesis and related diseases (e.g., NAFLD) (Kouroumalis et al., 2021; Trivedi et al., 2021; Zhou et al., 2022). Few studies focus on the relationship between folate and autophagy, especially on lipid metabolism in hepatocytes. Two studies on reproduction reported that dietary folate supplementation could improve rooster spermatogenesis and semen quality through autophagy in testis (Ye et al., 2022), and autophagy could be involved in abnormal mouse placentation due to folate deficiency (Yin et al., 2019). Another study found that folate supplementation could reduce LC3B expression in experimental NAFLD (Youssry and Kamel, 2019). Therefore, autophagy could play a role in the inhibition of hepatic lipogenesis by folate treatment.

ACKNOWLEDGMENTS

DISCLOSURES

The authors declare no conflict of interest.

SUPPLEMENTARY MATERIALS

Supplementary material associated with this article can be found in the online version at doi:10.1016/j.psj.2022.102363.

REFERENCES

Annibal, A., R. G. Tharyan, M. F. Schonewolff, H. Tam, C. Latza, M. M. K. Auler, S. Grönke, L. Partridge, and A. Antebi. 2021. Regulation of the one carbon folate cycle as a shared metabolic signature of longevity. Nat. Commun. 12:3486.

Christensen, K. E., L. G. Mikael, K. Y. Leung, N. Lévesque, L. Deng, Q. Wu, O. V. Malysheva, A. Best, M. A. Caudill, N. D. Greene, and R. Rozen. 2015. High folic acid consumption leads to pseudo-MTHFR deficiency, altered lipid metabolism, and liver injury in mice. Am. J. Clin. Nutr. 101:646–658.

Claire D'Andre, H., W. Paul, X. Shen, X. Jia, R. Zhang, L. Sun, and X. Zhang. 2013. Identification and characterization of genes that control fat deposition in chickens. J. Anim. Sci. Biotechnol. 4:43.

Cogburn, L. A., N. Trakooljul, C. Chen, H. Huang, C. H. Wu, W. Carré, X. Wang, and H. B. White 3rd. 2018. Transcriptional profiling of liver during the critical embryo-to-hatchling transition period in the chicken (Gallus gallus). BMC Genomics 19:695.

Crider, K. S., T. P. Yang, R. J. Berry, and L. B. Bailey. 2012. Folate and DNA methylation: a review of molecular mechanisms and the evidence for folate's role. Adv. Nutr. 3:21–38.

Da Silva, R. P., K. B. Kelly, A. Al Rajabi, and R. L. Jacobs. 2014. Novel insights on interactions between folate and lipid metabolism. Biofactors 40:277–283.

Ducker, G. S., and J. D. Rabinowitz. 2017. One-carbon metabolism in health and disease. Cell Metab. 25:27–42.

Fan, Y., B. N. Wolford, H. Lu, W. Liang, J. Sun, W. Zhou, O. Rom, A. Mahajan, I. Surakka, S. E. Graham, Z. Liu, H. Kim, S. Ramdas, L. G. Fritsche, J. B. Nielsen, M. E. Gabrielsen, K. Hveem, D. Yang, J. Song, M. T. Garcia-Barrio, J. Zhang, W. Liu, K. Zhang, C. J. Willer, and Y. E. Chen. 2021. Type 2 diabetes sex-specific effects associated with E167K coding variant in TM6SF2. iScience 24:103196.

Hebert, K., J. D. House, and W. Guenter. 2005. Effect of dietary folic acid supplementation on egg folate content and the performance and folate status of two strains of laying hens. Poult. Sci. 84:1533–1538.

Hu, J., B. Wang, and N. R. Sahyoun. 2016. Application of the key events dose-response framework to folate metabolism. Crit. Rev. Food Sci. Nutr. 56:1325–1333.

Huang da, W., B. T. Sherman, and R. A. Lempicki. 2009. Bioinformatics enrichment tools: paths toward the comprehensive functional analysis of large gene lists. Nucleic Acids Res. 37:1–13.

Kim, M., and B. H. Voy. 2021. Fighting fat with fat: n-3 polyunsaturated fatty acids and adipose deposition in broiler chickens. Front. Physiol. 12:755317.

Kintaka, Y., N. Wada, S. Shioda, S. Nakamura, Y. Yamazaki, and K. Mochizuki. 2020. Excessive folic acid supplementation in pregnant mice impairs insulin secretion and induces the expression of genes associated with fatty liver in their offspring. Heliyon 6:e03597.

Kouroumalis, E., A. Voumvouraki, A. Augoustaki, and D. N. Samonakis. 2021. Autophagy in liver diseases. World J. Hepatol. 13:6–65.

Kumar, K. A., A. Lalitha, D. Pavithra, I. J. Padmavathi, M. Ganeshan, K. R. Rao, L. Venu, N. Balakrishna, N. H. Shanker, S. U. Reddy, G. R. Chandak, S. Sengupta, and M. Raghunath. 2013. Maternal dietary folate and/or vitamin B12 restrictions alter body composition (adiposity) and lipid metabolism in Wistar rat offspring. J. Nutr. Biochem. 24:25–31.

Lam, T. Y., S. W. Seto, A. L. Au, C. C. Poon, R. W. Li, H. Y. Lam, W. S. Lau, S. W. Chan, S. M. Ngai, G. P. Leung, S. M. Lee, S. K. Tsui, and Y. W. Kwan. 2009. Folic acid supplementation modifies beta-adrenoceptor-mediated in vitro lipolysis of obese/diabetic (+db/+db) mice. Exp. Biol. Med. (Maywood) 234:1047–1055.

Langdon, W. B. 2015. Performance of genetic programming optimised Bowtie2 on genome comparison and analytic testing (GCAT) benchmarks. BioData Min. 8:1.

Leclerc, D., J. Jelinek, K. E. Christensen, J. J. Issa, and R. Rozen. 2021. High folic acid intake increases methylation-dependent expression of Lsr and dysregulates hepatic cholesterol homeostasis. J. Nutr. Biochem. 88:108554.

Lee, Y. S., S. Y. Kim, E. Ko, J. H. Lee, H. S. Yi, Y. J. Yoo, J. Je, S. J. Suh, Y. K. Jung, J. H. Kim, Y. S. Seo, H. J. Yim, W. I. Jeong, J. E. Yeon, S. H. Um, and K. S. Byun. 2017. Exosomes derived from palmitic acid-treated hepatocytes induce fibrotic activation of hepatic stellate cells. Sci. Rep. 7:3710.

Li, S., L. Zhi, Y. Liu, J. Shen, L. Liu, J. Yao, and X. Yang. 2016. Effect of in ovo feeding of folic acid on the folate metabolism, immune function and epigenetic modification of immune effector molecules of broiler. Br. J. Nutr. 115:411–421.

Lin, M. F., I. Jungreis, and M. Kellis. 2011. PhyloCSF: a comparative genomics method to distinguish protein coding and non-coding regions. Bioinformatics 27:i275–i282.

Liu, L., H. Cui, R. Fu, M. Zheng, R. Liu, G. Zhao, and J. Wen. 2017. The regulation of IMF deposition in pectoralis major of fast- and slow-growing chickens at hatching. J. Anim. Sci. Biotechnol. 8:77.

Liu, Y., X. Liu, J. Zhou, Z. Ren, X. Yang, Y. Cao, and X. Yang. 2019. Folic acid perfusion administration reduced abdominal fat deposition in starter Arbor Acres broilers. Poult. Sci. 98:6816–6825.

Liu, Y., J. Shen, X. Yang, Q. Sun, and X. Yang. 2018. Folic acid reduced triglycerides deposition in primary chicken hepatocytes. J. Agric. Food Chem. 66:13162–13172.

Liu, Y., L. Zhi, J. Shen, S. Li, J. Yao, and X. Yang. 2016. Effect of in ovo folic acid injection on hepatic IGF2 expression and embryo growth of broilers. J. Anim. Sci. Biotechnol. 7:40.

Liu, Y., J. Zhou, B. B. Musa, H. Khawar, X. Yang, Y. Cao, and X. Yang. 2020. Developmental changes in hepatic lipid metabolism of chicks during the embryonic periods and the first week of posthatch. Poult. Sci. 99:1655–1662.

Lyon, P., V. Strippoli, B. Fang, and L. Cimmino. 2020. B vitamins and one-carbon metabolism: implications in human health and disease. Nutrients 12:2867.

Moravcová, A., Z. Červinková, O. Kučera, V. Mezera, D. Rychtrmoc, and H. Lotková. 2015. The effect of oleic and palmitic acid on induction of steatosis and cytotoxicity on rat hepatocytes in primary culture. Physiol. Res. 64(Suppl. 5):S627–S636.

Na, W., Y. Y. Wu, P. F. Gong, C. Y. Wu, B. H. Cheng, Y. X. Wang, N. Wang, Z. Q. Du, and H. Li. 2018. Embryonic transcriptome and proteome analyses on hepatic lipid metabolism in chickens divergently selected for abdominal fat content. BMC Genomics 19:384.

Noble, R. C., and M. Cocchi. 1990. Lipid metabolism and the neonatal chicken. Prog. Lipid Res. 29:107–140.

Pan, Z., J. Wang, H. Tang, L. Li, J. Lv, L. Xia, C. Han, F. Xu, H. He, H. Xu, and B. Kang. 2011. Effects of palmitic acid on lipid metabolism homeostasis and apoptosis in goose primary hepatocytes. Mol. Cell. Biochem. 350:39–46.

Rao, S. V. R., M. Raju, T. Srilatha, D. Nagalakshmi, and U. Rajkumar. 2022. Supplementation of sulfur and folic acid improves performance of broiler chicken fed suboptimal concentrations of dietary methionine. J. Sci. Food Agric. 102:5720–5728.

Savaram, V. R. R., V. L. N. R. Mantena, S. S. Paul, N. Devanaboyina, S. Thota, P. Bhukya, and R. Ullengala. 2022. Enhancement of performance and anti-oxidant variables in broiler chicken fed diets containing sub-optimal methionine level with graded concentrations of sulphur and folic acid. Anim. Biosci. 35:721–729.

Siegel, P. B. 2014. Evolution of the modern broiler and feed efficiency. Annu. Rev. Anim. Biosci. 2:375–385.

Surugihalli, C., L. S. Farley, R. C. Beckford, B. Kamkrathok, H. C. Liu, V. Muralidaran, K. Patel, T. E. Porter, and N. E. Sunny. 2022. Remodeling of hepatocyte mitochondrial metabolism and de novo lipogenesis during the embryonic-to-neonatal transition in chickens. Front. Physiol. 13:870451.

Tibbetts, A. S., and D. R. Appling. 2010. Compartmentalization of mammalian folate-mediated one-carbon metabolism. Annu. Rev. Nutr. 30:57–81.

Trapnell, C., L. Pachter, and S. L. Salzberg. 2009. TopHat: discovering splice junctions with RNA-seq. Bioinformatics 25:1105–1111.

Trapnell, C., A. Roberts, L. Goff, G. Pertea, D. Kim, D. R. Kelley, H. Pimentel, S. L. Salzberg, J. L. Rinn, and L. Pachter. 2012. Differential gene and transcript expression analysis of RNA-seq experiments with TopHat and Cufflinks. Nat. Protoc. 7:562–578.

Trivedi, P., S. Wang, and S. L. Friedman. 2021. The power of plasticity-metabolic regulation of hepatic stellate cells. Cell Metab. 33:242–257.

Wang, L., H. J. Park, S. Dasari, S. Wang, J. P. Kocher, and W. Li. 2013. CPAT: Coding-Potential Assessment Tool using an alignment-free logistic regression model. Nucleic Acids Res. 41:e74.

Wu, S., W. Guo, X. Li, Y. Liu, Y. Li, X. Lei, J. Yao, and X. Yang. 2019. Paternal chronic folate supplementation induced the transgenerational inheritance of acquired developmental and metabolic changes in chickens. Proc. Biol. Sci. 286:20191653.

Xin, F. Z., Z. H. Zhao, R. N. Zhang, Q. Pan, Z. Z. Gong, C. Sun, and JG. Fan. 2020. Folic acid attenuates high-fat diet-induced steatohepatitis via deacetylase SIRT1-dependent restoration of PPARα. World J. Gastroenterol. 26:2203–2220.

Ye, N., Z. Lv, Z. Huang, Y. Cheng, Q. Wei, and F. Shi. 2022. Dietary folic acid supplementation improves semen quality and spermatogenesis through altering autophagy and histone methylation in the testis of aged broiler breeder roosters. Theriogenology 181:8–15.

Yin, X., R. Gao, Y. Geng, X. Chen, X. Liu, X. Mu, Y. Ding, Y. Wang, and J. He. 2019. Autophagy regulates abnormal placentation induced by folate deficiency in mice. Mol. Hum. Reprod. 25:305–319.

Youssry, S., and M. A. Kamel. 2019. Effect of folate supplementation on immunological and autophagy markers in experimental nonalcoholic fatty liver disease. Eur. Cytokine Netw. 30:135–143.

Yu, X., R. Liu, G. Zhao, M. Zheng, J. Chen, and J. Wen. 2014. Folate supplementation modifies CCAAT/enhancer-binding protein α methylation to mediate differentiation of preadipocytes in chickens. Poult. Sci. 93:2596–2603.

Zeng, X., M. Zhu, X. Liu, X. Chen, Y. Yuan, L. Li, J. Liu, Y. Lu, J. Cheng, and Y. Chen. 2020. Oleic acid ameliorates palmitic acid induced hepatocellular lipotoxicity by inhibition of ER stress and pyroptosis. Nutr. Metab. (Lond) 17:11.

Zhang, H., Q. Liang, N. Wang, Q. Wang, L. Leng, J. Mao, Y. Wang, S. Wang, J. Zhang, H. Liang, X. Zhou, Y. Li, Z. Cao, P. Luan, Z. Wang, H. Yuan, Z. Wang, X. Zhou, S. J. Lamont, Y. Da, R. Li, S. Tian, Z. Du, and H. Li. 2020. Microevolutionary dynamics of chicken genomes under divergent selection for adiposity. iScience 23:101193.

Zhang, Y., N. Zhang, L. Liu, Y. Wang, J. Xing, and X. Li. 2021. Transcriptome analysis of effects of folic acid supplement on gene expression in liver of broiler chickens. Front. Vet. Sci. 8:686609.

Zhou, J. C., J. L. Wang, H. Z. Ren, and X. L. Shi. 2022. Autophagy plays a double-edged sword role in liver diseases. J. Physiol. Biochem. 78:9–17.